Chemico-Biological Interactions 323 (2020) 109074

Contents lists available at ScienceDirect

Chemico-Biological Interactions

journal homepage: www.elsevier.com/locate/chembioint

MAY, a novel tubulin inhibitor, induces cell apoptosis in A549 and A549/Taxol cells and inhibits epithelial-mesenchymal transition in A549/Taxol cells

Jianan Du[a], Jingnan Li[a], Minghuan Gao[a], Qi Guan[b], Tong Liu[a], Yue Wu[b], Zengqiang Li[a], Daiying Zuo[a,*], Weige Zhang[b,**], Yingliang Wu[a,***]

[a] Department of Pharmacology, Shenyang Pharmaceutical University, 103 Wenhua Road, Shenhe District, Shenyang, 110016, China
[b] Key Laboratory of Structure-Based Drug Design and Discovery, Ministry of Education, Shenyang Pharmaceutical University, 103 Wenhua Road, Shenhe District, Shenyang, 110016, China

ARTICLE INFO

Keywords:
Apoptosis
Multidrug resistance
Epithelial-mesenchymal transition
P-glycoprotein
MAY

ABSTRACT

Non-small-cell lung cancer (NSCLC) is one of the common malignant tumors, and multidrug resistance (MDR) and tumor metastasis limit the anticancer effect of NSCLC. Therefore, it is necessary to develop new anticancer drug that can inhibit MDR and metastasis of NSCLC. In the present study, we found that 5-(2-chlorophenyl)-4-(4-(3,5-dimethoxyphenyl)piperazine-1-carbonyl)-2*H*-1,2,3- triazole (MAY) displayed strong cytotoxic effect on A549 and taxol-resistant A549 cells (A549/Taxol cells). We further discovered that MAY led to G2/M phase arrest by inhibiting microtubule polymerization in both cells. Then MAY caused apoptosis by the mitochondrial pathway in A549 cells and through the extrinsic pathway in A549/Taxol cells. Interestingly, MAY was not a substrate for P-glycoprotein (P-gp), which was highly expressed in A549/Taxol cells, and MAY inhibited the expression and efflux function of P-gp. Furthermore, MAY inhibited epithelial-mesenchymal transition (EMT) by targeting Twist1 in A549/Taxol cells. In summary, our results suggest that MAY induces apoptosis in A549 and A549/Taxol cells and inhibits EMT in A549/Taxol cells. These findings suggest that MAY could provide a promising method for the treatment of NSCLC, especially for the treatment of resistant NSCLC.

1. Introduction

Non-small-cell lung cancer (NSCLC) has increasing rates of incidence and has become one of the most prevalent malignant tumors [1–4]. Chemotherapy is one of the most valid methods and paclitaxel is the most commonly used drug for the clinical treatment of NSCLC [5–7]. However, resistance to paclitaxel reduces the efficacy of chemotherapy and limits its clinical application.

Many studies on multidrug resistance (MDR) have revealed the resistant mechanisms of drugs, including change of drug target structure, repair of DNA damage, and the most important one is enhancing the function of ATP-binding cassette transporters (ABC transporters) [8–11]. P-glycoprotein (P-gp), an ABC transporter, can decrease the concentration of drugs by pumping them out of the cells and inhibit the efficacy of drugs [12–14]. Thus, suppressing the function of P-gp is the main method to overcome chemotherapy resistance.

Epithelial-mesenchymal transition (EMT) is a reversible biological process and plays an important role in the malignant development of tumors [15,16]. EMT can not only strengthen the motility of tumor cells, but also give them stem cell characteristics [17]. Studies have shown that EMT can lead to increase of the expression and function of ABC transporters, causing chemoresistance in cancers [16,18,19]. Many studies show that EMT transcription factors (EMT-TFs) regulate the pumping function of ABC transporters and EMT process in a variety of tumor cells [20–23]. Therefore, it is of great important to develop chemotherapeutic agent that can inhibit EMT and drug resistance.

A series of microtubule inhibitors have been synthesized by our group. Among them, 5-(2-chlorophenyl)-4-(4-(3,5-dimethoxyphenyl) piperazine-1-carbonyl)-2*H*- 1,2,3-triazole (MAY) (Fig. 1a) was identified as a colchicine binding site inhibitor of tubulin and can strongly suppress microtubule polymerization in SGC-7901 cells [24]. In the present study, MAY exhibited cytotoxic effect on various cancer cells,

* Corresponding author.
** Corresponding author.
*** Corresponding author.
E-mail addresses: zuodaiying@163.com (D. Zuo), zhangweige2000@sina.com (W. Zhang), yingliang_1016@163.com (Y. Wu).

https://doi.org/10.1016/j.cbi.2020.109074
Received 13 January 2020; Received in revised form 9 March 2020; Accepted 21 March 2020
Available online 23 March 2020

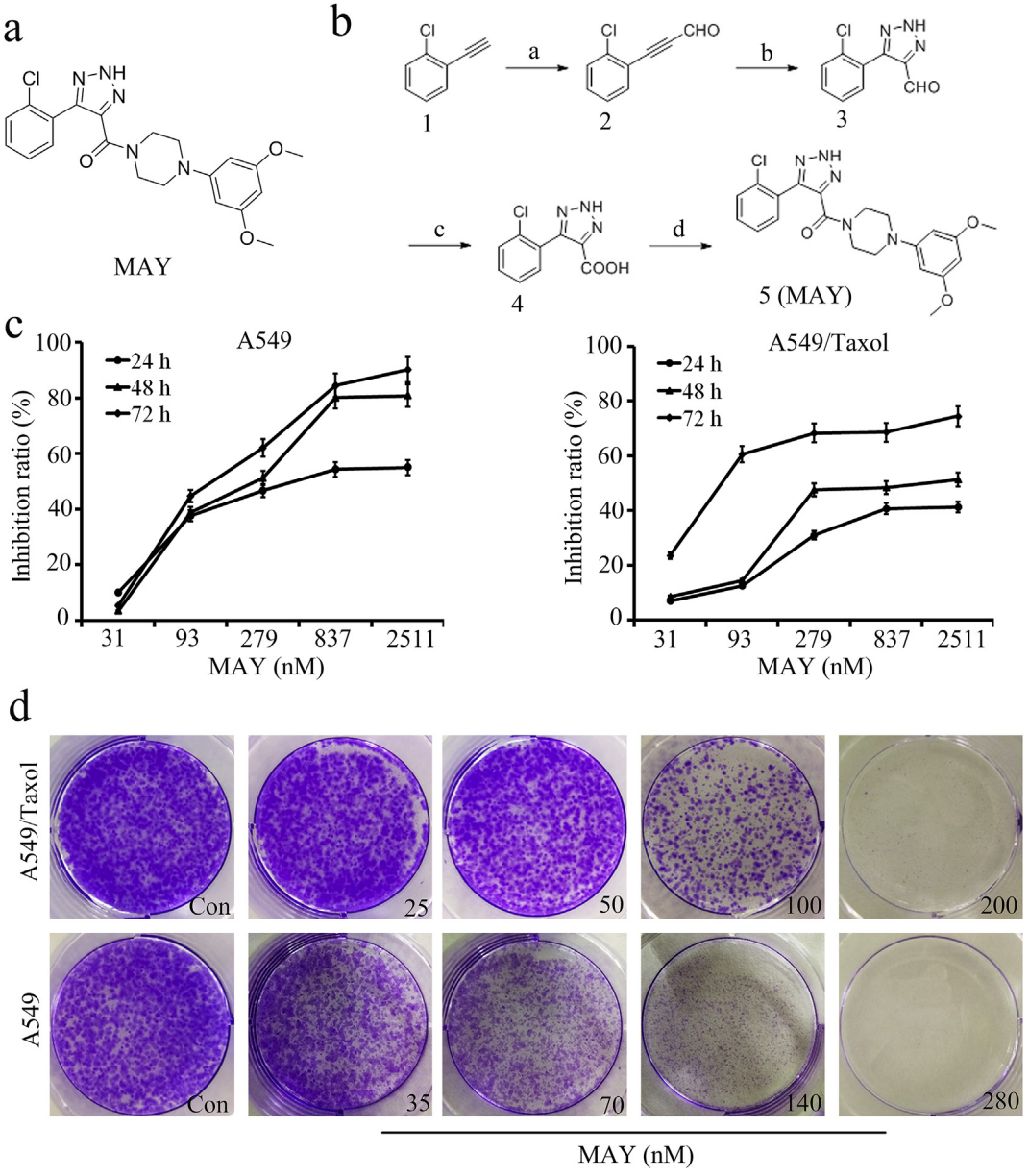

Fig. 1. Effects of MAY on A549 and A549/Taxol cell viability and proliferation. (a) The chemical structure of MAY. (b) Synthetic route of MAY. Reagents and conditions: a. 1) n-BuLi (2.5 M in hexane), THF, −40 ℃, 30 min; 2) DMF, −40 ℃, 3) r.t., 1 h; b. NaN3, DMSO, r.t., 30 min; c. H_2O_2, KOH, MeOH, 30 min; d. arylpiperazine, EDCI, HOBt, ethyl acetate, r.t., overnight. (c) Cell viabilities of A549 and A549/Taxol cells were detected by the MTT assay after treatment with MAY for 24, 48 and 72 h. (d) The growth inhibition effects of MAY on A549 and A549/Taxol cells were measured by colony formation assay.

particularly taxol-resistant A549 cells (A549/Taxol cells). MAY induced apoptosis in A549 and A549/Taxol cells and inhibited EMT in A549/Taxol cells. However, the detailed mechanism has not been described. In this study, we intend to clarify the mechanisms by which MAY induces apoptosis and inhibits EMT. This will provide an evidence for MAY as a potential agent to treat paclitaxel-resistant NSCLC.

2. Materials and methods

2.1. Materials

MAY was synthesized by our laboratory. The synthetic route was outlined in Fig. 1b. 1-Chloro-2-ethynylbenzene (**1**) was used as the starting material, which was converted into 3-(2-chlorophenyl)propiolaldehyde (**2**) by the formylation reaction. Then, a thermal azide-alkyne 1,3-dipolar cycloaddition was carried out for obtaining 5-(2-chlorophenyl)-2*H*-1,2,3-triazole-4-carbaldehyde (**3**), followed by oxidation to 5-(2-chlorophenyl)-2*H*-1,2,3-triazole-4-carboxylic acid (**4**) with hydrogen peroxide. Finally, amidation was carried by 1-Ethyl-3-(3-dimethyl laminopropyl)carbodiie hydrochlide (EDCI) and Nhydroxybenzotrizole (HOBt) to generate the desired compound 5-(2-chlorophenyl)-4-(4-(3,5-dimethoxyphenyl)piperazine-1-carbonyl)-2*H*−1,2,3-triazole (**5**, MAY). The MAY was purified by column chromatography, and the purity was more than 98% by HPLC method. The data of HRMS and NMR spectroscopy are in agreement with our previous study [24]. Combretastain A-4 (CA-4), Taxol, doxorubicin (ADM) and verapamil (VRP) were purchased from Sigma Chemical (St. Louis, MO, USA). MTT and propidium iodide (PI) were purchased from Sigma-Aldrich (St. Louis, MO, USA). Hoechst 33342, BCA protein assay kit, crystal violet and Rhodamine123 (Rh123) were purchased from Beyotime Biotechnology (Nanjing, P.R.C). Annexin V-FITC/PI staining kit was purchased from KeyGEN BioTECH (Nanjing, China). Primary

Table 1
IC_{50} of MAY against various human cancer cell lines (mean ± SD, n = 3).

Tumor type	Cell line	IC_{50} (nM)
Stomach	**SGC-7901**	**95.5 ± 1.5**
Liver	**HepG2**	**149.5 ± 3.5**
	BEL-7402	**89.0 ± 1.5**
Cervix	**HeLa**	**81.0 ± 7.5**
Breast	**MCF-7**	**96.5 ± 1.5**
	MCF-7/ADR	**295.7 ± 3.7**
Lung	**A549**	**67.0 ± 2.5**
	A549/Taxol	**52.0 ± 1.0**

antibodies against α-tubulin, CyclinB1, Cdc2, CDK7 and HRP-conjugated and FITC-conjugated secondary antibodies were purchased from Santa Cruz Biotechnology (Delaware Ave Santa Cruz, CA, USA). P-gp, matrix metalloprotein 2 (MMP2) and β-actin antibodies were purchased from Bioss (Beijing, P.R.C). Bax, Bcl-2, PARP, caspase 3, caspase 8, caspase 9, E-cadherin, N-cadherin, Vimentin, Snail1, Twist1 and matrix metalloprotein 9 (MMP9) antibodies were obtained from Proteintech (Chicago, IL, USA). Primary antibodies against FAS and FASL were obtained from Wanleibio (Shenyang, China).

2.2. Cell culture

A549, HepG2, SGC-7901, HeLa, BEL-7402, MCF-7 and adriamycin-resistant MCF-7 (MCF-7/ADR) cells were purchased from the Shanghai Institute of Cell Resource Center Life Science (Shanghai, China). Taxol-resistant A549 (A549/Taxol) cells were obtained from Professor Yang (Shenyang Pharmaceutical University). All cells were cultured in RPMI 1640 or DMEM containing 10% fetal bovine serum at 37 °C and 5% CO_2.

2.3. Cell viability

Growth inhibition of tumor cells was examined by the MTT assays [25]. Briefly, cells were seeded in 96-well plates at a density of 3000–5000 cells/well and incubated overnight. The cells were treated with compounds or medium for different times and 20 μl MTT was added to per well. After incubation for 4 h, the supernatant was removed and 150 μl DMSO was added. Finally, the absorbance was measured at 420 nM by a microplate reader (MK3, Thermo, Germany). The resistance index (RI) was the ratio of the IC_{50} of the resistant cells to that of parental cells.

2.4. Colony formation assay

Cells were seeded in six-well plates at a density of 6000 cells/well and incubated overnight. After treatment with different concentrations of MAY or medium for 48 h, the original medium was removed and replaced with the drug-free medium. After incubation for 7 days, cells were fixed with 4% paraformaldehyde for 20 min and stained with crystal violet for 15 min, then photographed by a camera (Canon, Tokyo, Japan).

2.5. Immunofluorescence staining

Cells were seeded in six-well plates with glass coverslips and treated with MAY or medium for 24 h. Then the cells were incubated overnight at 4 °C with the primary antibodies and incubated with FITC-conjugated secondary antibodies at room temperature for 3 h. Nuclei were stained with DAPI. Images were photographed using confocal microscope (Nikon C2, Tokyo, Japan).

Table 2
The resistance index (RI) for various compounds in A549/Taxol cells (mean ± SD, n = 3).

Compounds	IC_{50} (nM)		RI
	A549	A549/Taxol	
Taxol	**20.3 ± 3.1**	**6992.4 ± 266.2**	**344.5**
ADM	**135.5 ± 21.2**	**968.7 ± 193.3**	**7.2**
CA-4	**24.2 ± 1.8**	**988.4 ± 95.9**	**40.8**
MAY	**67.0 ± 2.5**	**52.0 ± 1.0**	**0.7**

2.6. Cell cycle analysis

Cells were incubated with MAY or medium for the different times, then the cells were collected and fixed in 70% ice ethanol. Next, the cells were stained with PI for 30 min. Finally, the cells were detected by FACS (BD Biosciences, NY, USA).

2.7. Hoechst staining

Cells were seeded in six-well plates at a density of 1.5×10^4 cells/well and incubated overnight. And cells were treated with MAY or CA-4 for different times. Then the cells were stained with Hoechst 33342. Images were photographed using fluorescence microscope (Olympus, Tokyo, Japan).

2.8. Cell apoptosis analysis

Cell apoptosis was detected by Annexin V-FITC/PI staining kit. Cells were treated with MAY or CA-4 for the indicated times and collected. Then the cells were stained based on the kit instructions. Samples were detected by FACS (BD Biosciences, NY, USA).

2.9. Mitochondrial membrane potential analysis

Changes in mitochondrial transmembrane potential as a result of mitochondrial perturbation were measured after staining with Rh123 [26]. Cells were incubated with MAY for different times, then the cells were stained with Rh123 in the dark for 30 min at 37 °C. Samples were detected by FACS (BD Biosciences, NY, USA).

2.10. Wound healing assay

Wound healing assay was conducted based on previous description [17]. Concisely, cells were seeded in six-well plates and incubated overnight. Wounds were formed by scraping with pipette tips, then the cells were washed with PBS and the medium with or without MAY was added. Images were photographed at 48 h by a microscope (Olympus, Tokyo, Japan).

2.11. Transwell migration and invasion assays

Cells seeded in the upper chamber (Corning, NY, USA) were incubated with serum-free medium and medium with 10% FBS was added to the lower chamber. After being incubated with MAY or medium for 48 h, the cells migrated on the lower membrane were fixed and stained. Invasion assay was similar to the description except adding the matrigel (BD Bioscience, NY, USA) to the upper chamber.

2.12. Intracellular Rh123 accumulation assay

Cells were seeded in six-well plates at a density of 1.0×10^4 cells/well and incubated overnight. Cells were treated with or without MAY and co-incubated with 15 mM Rh123 in the dark for 48 h. Samples were detected by FACS (BD Biosciences, NY, USA).

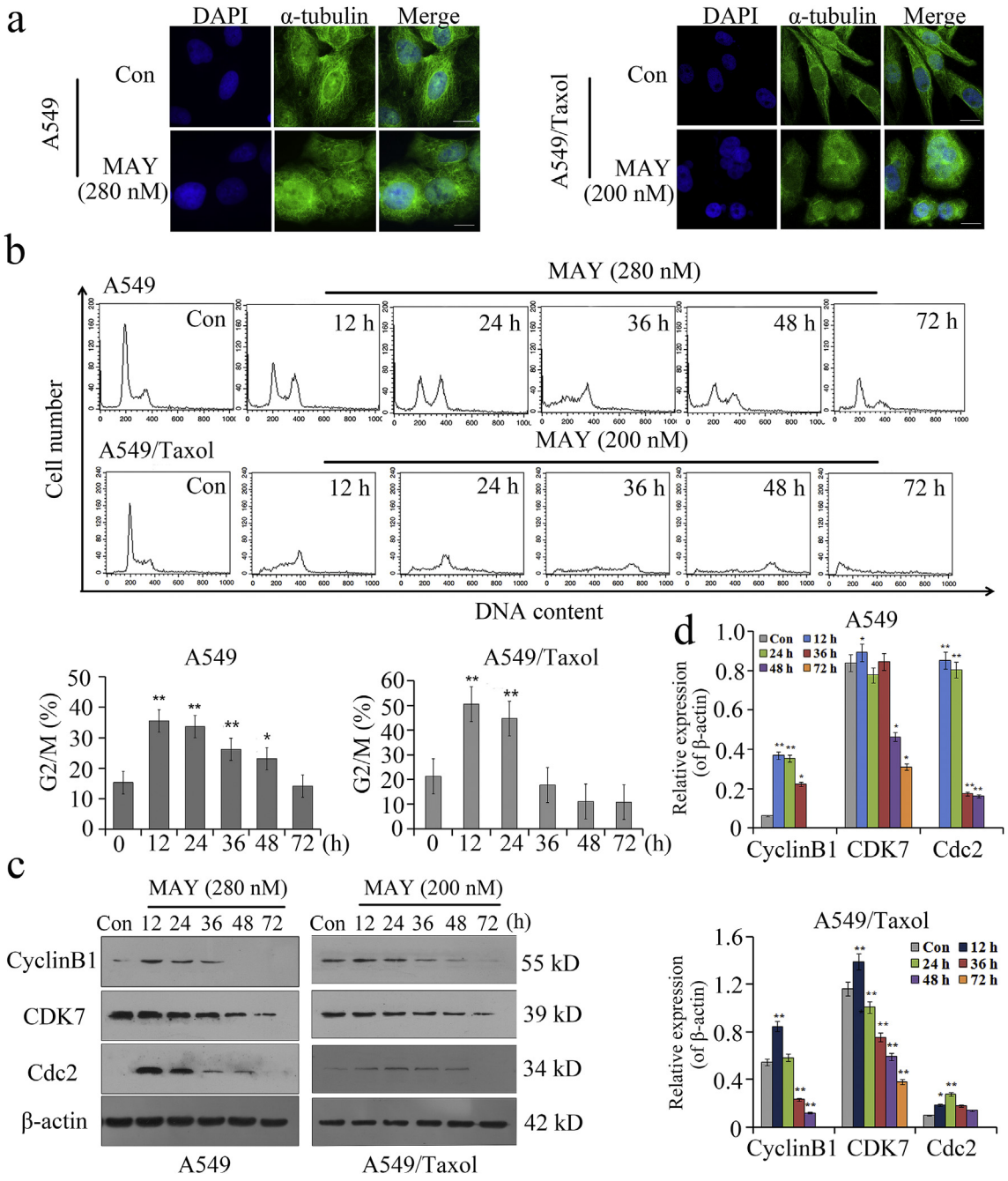

Fig. 2. MAY inhibits microtubule polymerization and induces G2/M phase arrest. (a) Immunofluorescence analysis showed microtubule distribution in A549 and A549/Taxol cells with MAY (280 and 200 nM, respectively) treatment for 24 h. Scale bar = 10 μm. (b) FACS analysis showed the cell cycle distribution in A549 and A549/Taxol cells after treatment with MAY (280 and 200 nM, respectively) for the indicated times. (c) and (d) Western blot showed the expression changes of cell cycle-related proteins in MAY-treated A549 and A549/Taxol cells. *$p < 0.05$, **$p < 0.01$ *vs* control.

2.13. Western blot analysis

Western blot was conducted according to the previous description [25]. Concisely, the protein samples were separated on polyacrylamide gels and transferred to PVDF membranes. Then the membranes were incubated with the primary antibodies at 4 °C overnight and the HRP-conjugated secondary antibodies at room temperature for 3 h. Proteins were visualized using enhanced chemiluminescence (ECL) reagent. Densitometry analysis was performed using Image J software.

2.14. Statistical analysis

All experiments were performed three times and the data were expressed as mean ± SD. All statistical analysis was performed by one-way analysis of variance (ANVOA) and LSD tests using SPSS 22.0 software. *p*-values < 0.05 were considered to be statistically significant.

3. Results

3.1. MAY shows effective cytotoxic effect on multiple cancer cells

The MTT assays revealed that MAY inhibited the growth of multiple

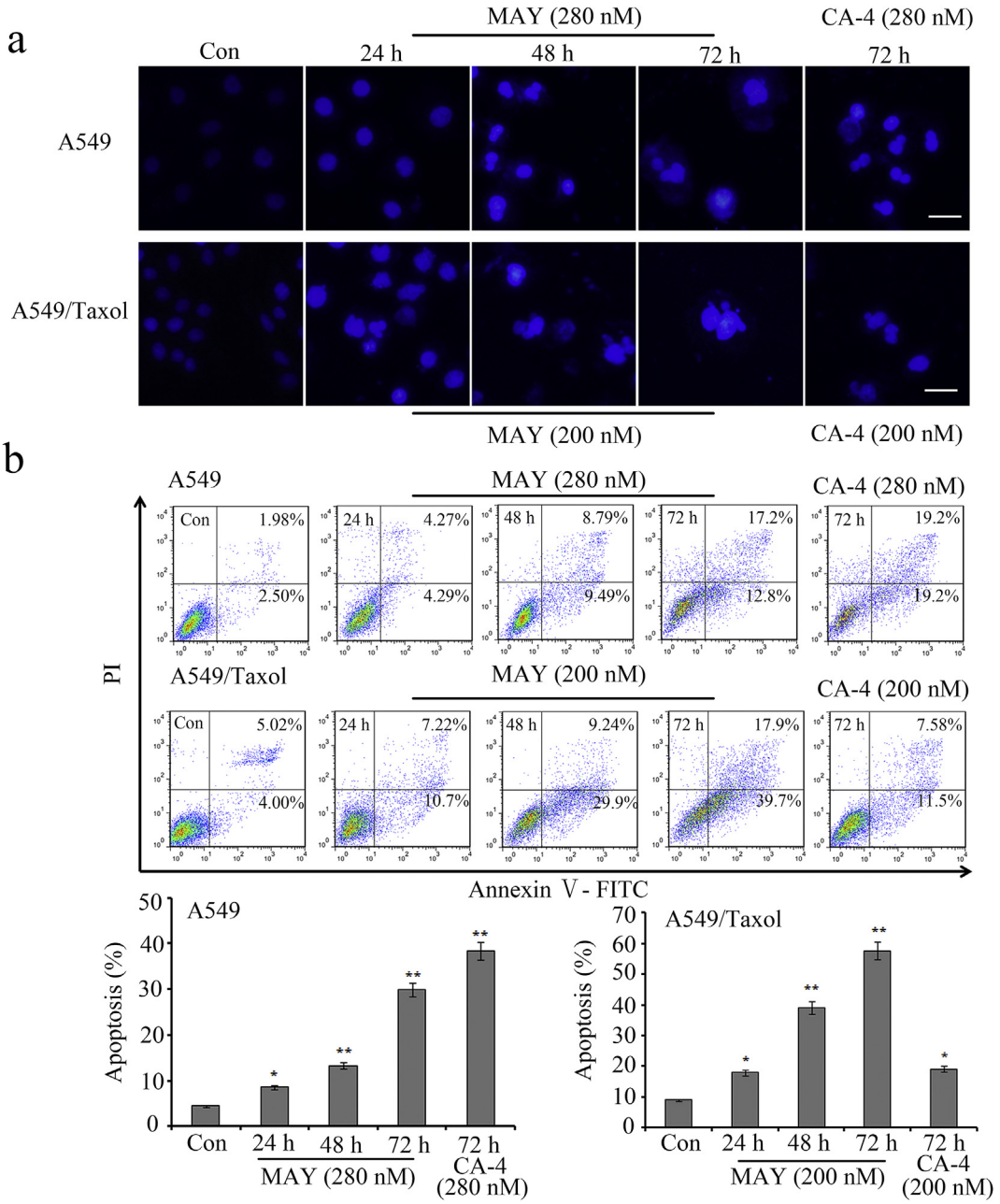

Fig. 3. MAY induces apoptosis in A549 and A549/Taxol cells. (a) The changes of nuclei were detected by Hoechst 33342 staining. Scale bar = 10 μm. (b) FACS analysis showed MAY (280 and 200 nM, respectively) induced apoptosis in A549 and A549/Taxol cells. *$p < 0.05$, **$p < 0.01$ *vs* control.

cancer cells, such as A549, A549/Taxol, HepG2, SGC-7901, HeLa, BEL-7402, MCF-7 and MCF-7/ADR cells, indicated that MAY had broad spectrum anti-tumor activity (Table 1). Interestingly, ADM, paclitaxel and CA-4 significantly inhibited A549 cells but weakly inhibited A549/Taxol cells. However, MAY had a stronger inhibitory effect on A549/Taxol cells compared with A549 cells, and the RI was 0.7 (Table 2). The MTT assays revealed that MAY suppressed the growth of A549 and A549/Taxol cells in time- and concentration-dependent manners (Fig. 1c). Next, we detected cell proliferation by colony formation assay. The results indicated that MAY inhibited the ability of colony formation in concentration-dependent manners in A549 and A549/Taxol cells (Fig. 1d).

3.2. MAY inhibits microtubule polymerization and induces G2/M phase arrest in A549 and A549/Taxol cells

We observed the changes of intracellular microtubule network by immunofluorescence assay. The results showed that the microtubules were obviously depolymerized and the fragments were dispersed in the cytoplasm after MAY treatment for 24 h, whereas the untreated cells exhibited intact and clear microtubules in both A549 and A549/Taxol cells (Fig. 2a). Studies have shown that microtubule inhibitors usually cause cell cycle arrest [27,28]. Cell cycle assays showed that MAY treatment for 12 h led to cell accumulation in the G2/M phase in both A549 and A549/Taxol cells (Fig. 2b). Next, we examined the key molecules during the G2/M phase by western blot. The results indicated that MAY significantly increased the expression of CyclinB1, CDK7 and Cdc2 at 12 h in A549 and A549/Taxol cells (Fig. 2c and d). Above data indicated that MAY induced G2/M phase arrest in both A549 and

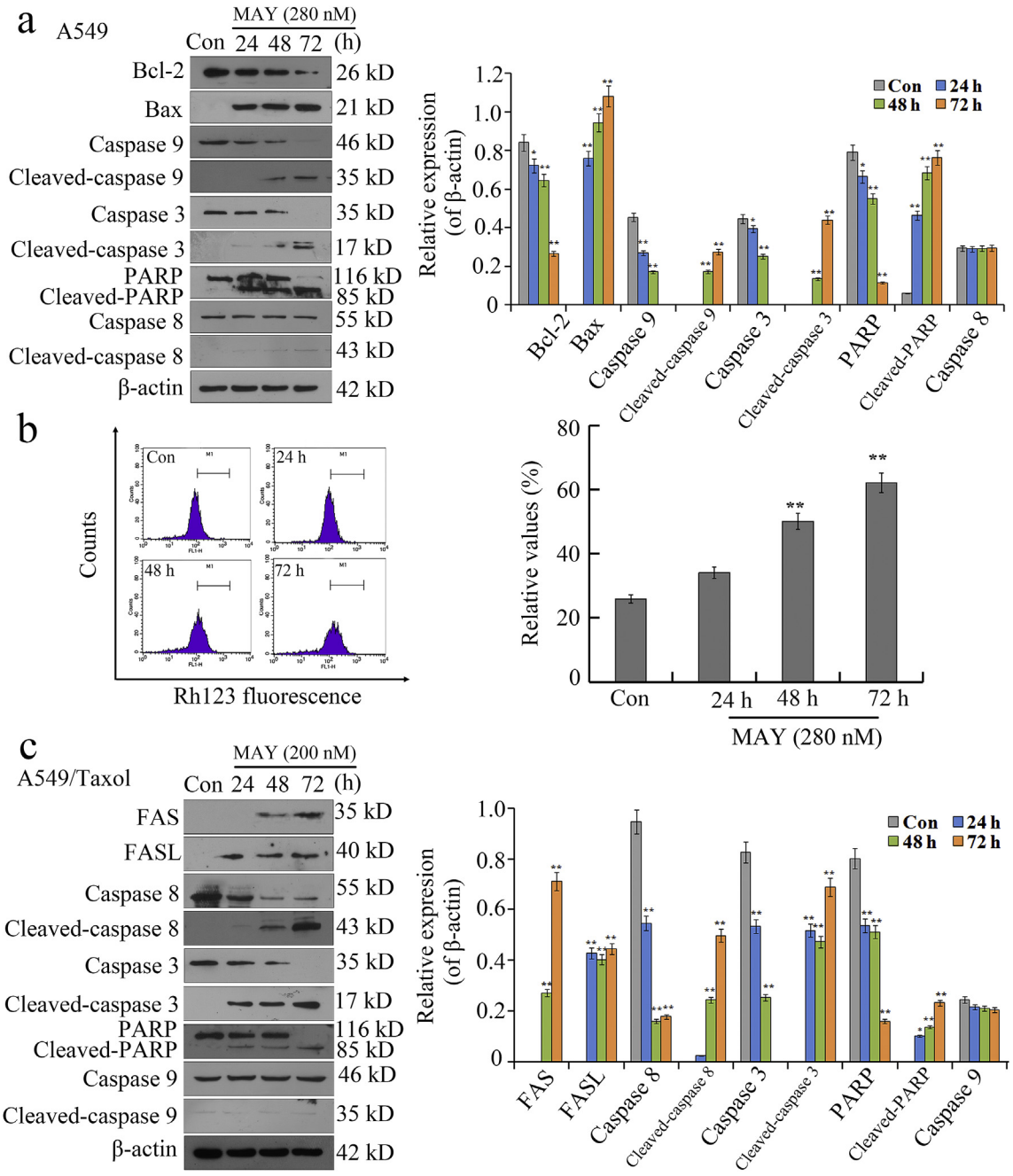

Fig. 4. MAY induces apoptosis through the intrinsic pathway in A549 cells and through the extrinsic pathway in A549/Taxol cells. (a) Western blot showed the expression of apoptosis-related protein in MAY (280 nM)-treated A549 cells. (b) FACS analysis showed the mitochondrial membrane potential of A549 cells after treatment with MAY (280 nM) for 24, 48 and 72 h. (c) Western blot showed the expression of apoptosis-related protein in MAY (200 nM)-treated A549/Taxol cells. $^{*}p < 0.05$, $^{**}p < 0.01$ *vs* control.

A549/Taxol cells.

3.3. MAY induces apoptosis through the mitochondrial pathway in A549 cells and through the extrinsic pathway in A549/Taxol cells

The above data showed that MAY suppressed the growth of NSCLC cells and induced G2/M phase arrest, so we explored whether MAY induced apoptosis. First of all, we observed the changes of nuclei by Hoechst 33342 staining. A549 and A549/Taxol cells were stained evenly and the nucleus edge was neat and round in the control group. After treatment with MAY, the cells were stained in bright blue, the nuclei were expanded and apoptotic bodies were obvious (Fig. 3a). As shown in Fig. 3b, MAY induced apoptosis in A549 and A549/Taxol cells in time-dependent manners. Furthermore, the results showed that the effect of MAY was significantly stronger than that of CA-4 at same concentration in A549/Taxol cells. Next, in order to explore the way of apoptosis in A549 and A549/Taxol cells, we conducted the following experiments. As shown in Fig. 4a, MAY decreased the expression of Bcl-2, caspase 9, caspase 3 and PARP and strengthened the expression of Bax, cleaved-caspase 9, cleaved-caspase 3 and cleaved-PARP in time-dependence manners in A549 cells. However, the expression of caspase 8 had almost no change and there was no detectable cleaved-caspase 8 expression. In A549 cells, after treatment with MAY, the extracellular Rh123 fluorescence intensity was increased, indicating that the intracellular mitochondrial membrane potential was decreased (Fig. 4b). Above results revealed that MAY induced apoptosis in A549 cells

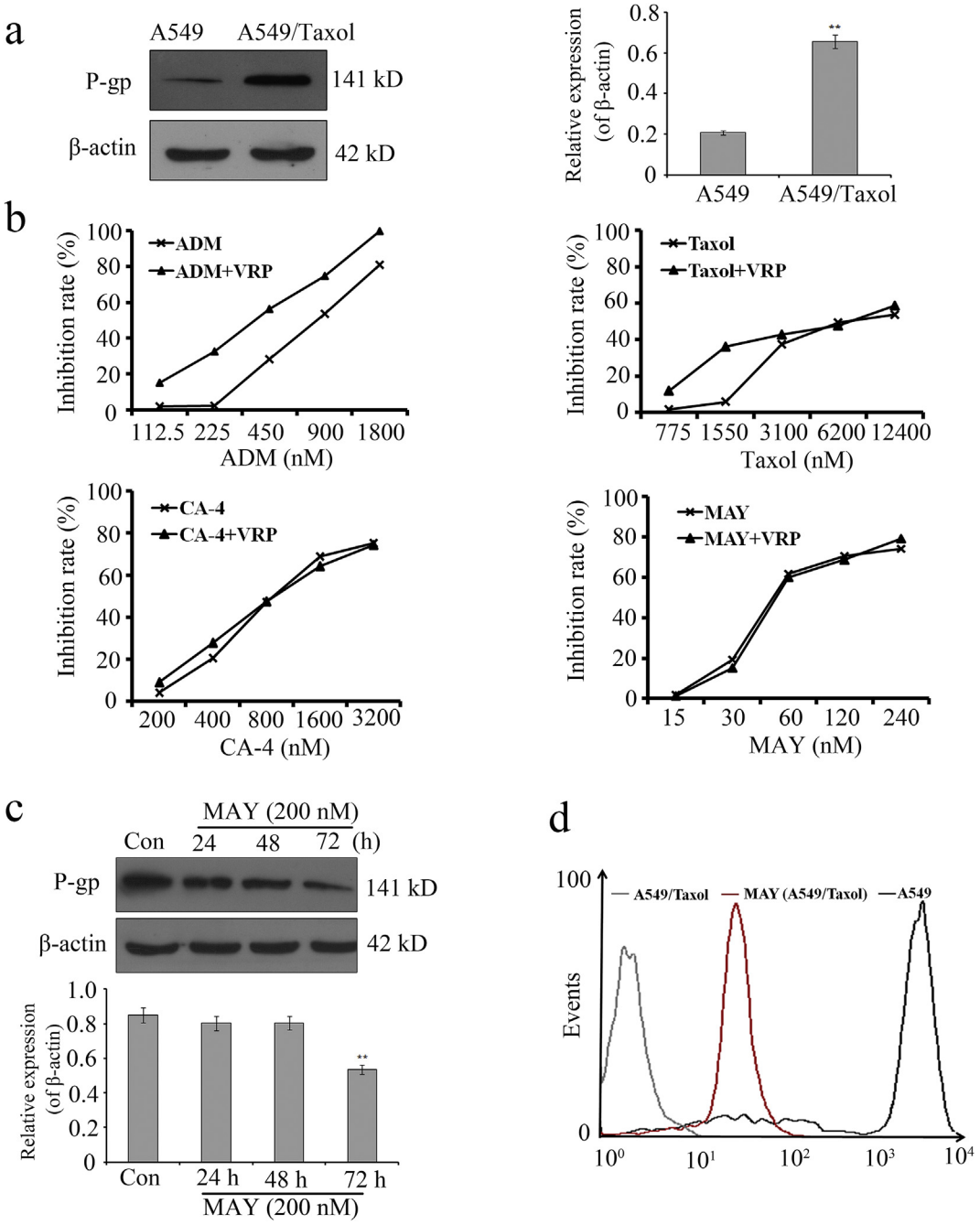

Fig. 5. MAY inhibits P-gp expression and function in A549/Taxol cells. (a) Western blot showed the expression of P-gp in A549 and A549/Taxol cells. (b) Cell viabilities of A549/Taxol cells were detected by the MTT assays after treatment with different concentrations of compounds alone or combined with VRP (10 mM) for 72 h. (c) Western blot showed the expression of P-gp in MAY (200 nM)-treated A549/Taxol cells. (d) The accumulation of Rh123 was measured by FACS analysis. *$p < 0.05$, **$p < 0.01$ *vs* control.

through the intrinsic pathway. Then, we examined the expression of apoptosis-related proteins in A549/Taxol cells by western blot. The results showed that MAY decreased the expression of caspase 8, caspase 3 and PARP and up-regulated the expression of FAS, FASL, cleaved-caspase 8, cleaved-caspase 3 and cleaved-PARP in time-dependence manners in A549/Taxol cells. However, there was little change in the expression of caspase 9 and there was no detectable cleaved-caspase 9 expression (Fig. 4c). These results revealed that MAY induced apoptosis in A549/Taxol cells through the extrinsic pathway.

3.4. MAY inhibits P-gp expression and function in A549/Taxol cells

P-gp pumping drugs out of cells to reduce drug concentration is one of the main causes of chemotherapy resistance in tumor cells [29]. Immunoblotting analysis showed that P-gp was highly expressed in A549/Taxol cells compared with A549 cells (Fig. 5a). Most drugs targeting tubulins are substrates of P-gp, which are pumped out of cells by P-gp, resulting in drug resistance [30]. To investigate whether MAY was a substrate of P-gp, we examined the effects of several drugs on A549/Taxol cell viabilities by co-incubating these drugs with VRP. The growth inhibition of A549/Taxol cells showed that VRP enhanced the inhibition effect of taxol and ADM, which are typical substrates of P-gp,

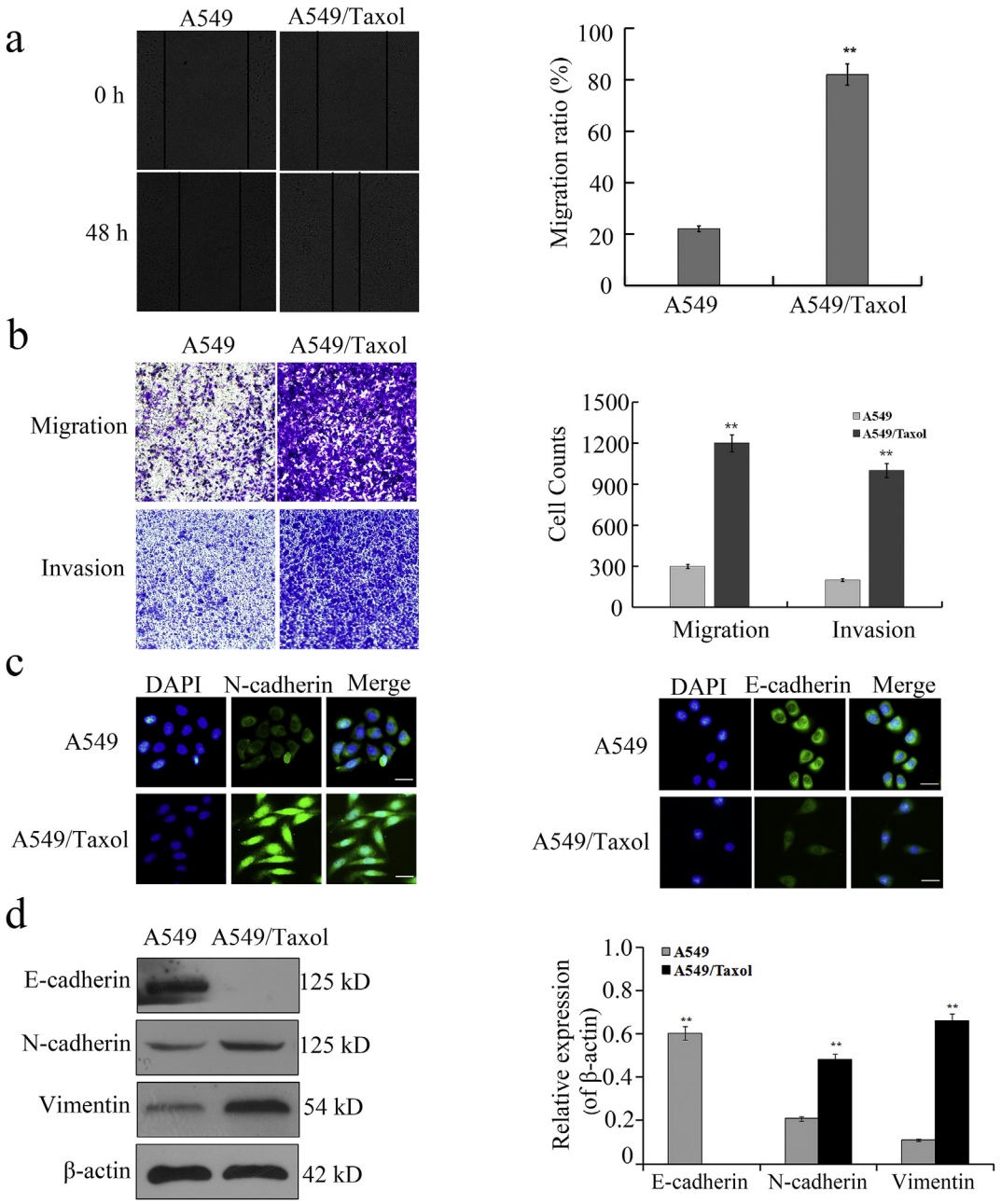

Fig. 6. EMT features in A549/Taxol cells. (a) Wounding healing assay showed the motility of A549 and A549/Taxol cells. (b) Transwell assays showed crystal violet stained A549 and A549/Taxol cells on the insert membranes after incubation for 48 h. (c) Immunofluorescence showed the expression of epithelial marker (E-cadherin) and mesenchymal marker (N-cadherin) in A549 and A549/Taxol cells. Scale bars = 50 μm. (d) Western blot showed the expression levels of Ecadherin, N-cadherin and Vimentin in A549 and A549/Taxol cells. $*p < 0.05$, $**p < 0.01$ *vs* A549 cells.

whereas VRP did not affect the inhibitory effect of CA-4 and MAY (Fig. 5b), which indicates that MAY is not a substrate for P-gp. In addition, MAY significantly reduced the expression of P-gp in time-dependence manners in A549/Taxol cells (Fig. 5c). Next, we detected the intracellular accumulation of P-gp fluorescent substrate Rh123. As shown in Fig. 5d, Rh123 levels in A549 cells were much higher than those in A549/Taxol cells. Interestingly, MAY could lead to intracellular Rh123 accumulation in A549/Taxol cells, which indicates that MAY can inhibit P-gp function in A549/Taxol cells (Fig. 5d).

3.5. EMT is distinct in A549/Taxol cells

We observed that A549 cells were in a flat form, while A549/Taxol cells were transformed into elongated shape, suggesting that cells may exhibit EMT-like changes. Because of the relationship between EMT and cell motility, we analyzed the ability of metastasis in A549/Taxol cells. The wound healing assay indicated that drug resistance enhanced cell motility (Fig. 6a). The migration and invasion assays showed the same results (Fig. 6b). Moreover, in order to demonstrate whether A549/Taxol cells occur EMT, we investigated the expression of EMT-related markers. Immunofluorescence indicated that the mesenchymal marker N-cadherin was increased and the epithelial marker E-cadherin was reduced in A549/Taxol cells compared with A549 cells (Fig. 6c). As shown in Fig. 6d, E-cadherin in A549/Taxol cells was significantly reduced compared with A549 cells. However, N-cadherin and Vimentin were increased significantly in A549/Taxol cells. Together, above results showed that A549/Taxol cells underwent EMT.

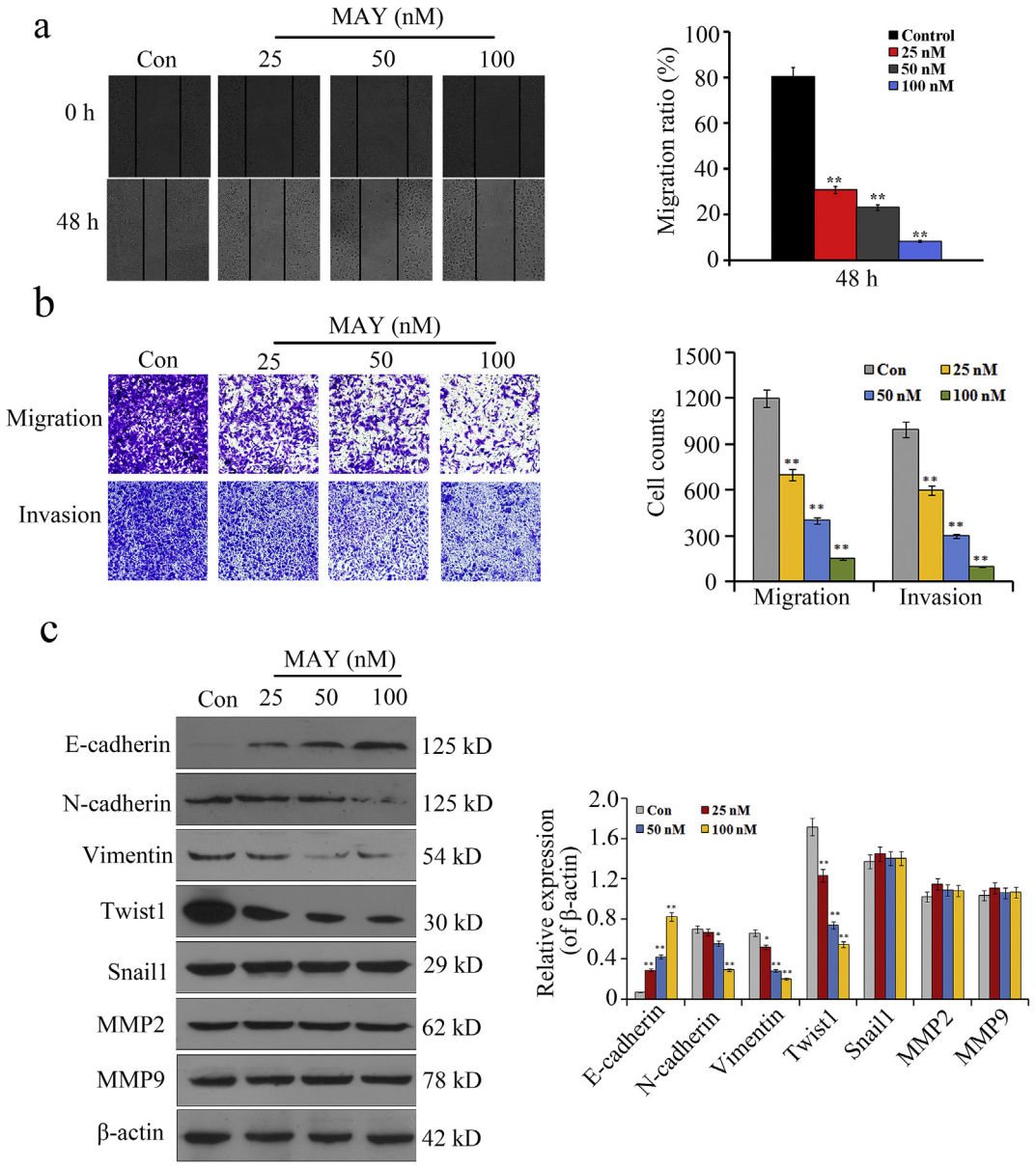

Fig. 7. MAY inhibits EMT by targeting Twist1 in A549/Taxol cells. (a) Wounding healing assay showed the motility of A549/Taxol cells treated with MAY for 48 h. (b) Transwell assays showed crystal violet stained A549/Taxol cells treated with MAY treatment for 48 h. (C) Western blot showed the expression of EMT-related proteins in MAY- treated A549/Taxol cells. $*p < 0.05$, $**p < 0.01$ *vs* control.

3.6. MAY inhibits EMT by targeting Twist1 in A549/Taxol cells

Drugs targeting microtubules affect the ability of cell motility [31]. Therefore, we explored the influence of MAY on A549/Taxol cell motility. When the inhibition rate of a drug on cells is less than 10%, it indicates that there is no significant cytotoxic effect on the cells [32]. The inhibition rate of A549/Taxol cells by MAY (100 nM) treatment for 48 h was about 10%, so we chose 100 nM as the maximum concentration for the following experiments. The results indicated that MAY suppressed the migration and invasion of A549/Taxol cells in concentration-dependent manners (Fig. 7a and b). Western blot indicated that MAY enhanced the expression of E-cadherin and inhibited the expression of N-cadherin and Vimentin (Fig. 7c). These results indicated that MAY inhibited EMT in A549/Taxol cells. To further investigate the potential molecular mechanisms, we examined the expression of EMT-TFs by western blot. The results revealed that MAY significantly reduced the expression of Twist1 and almost had no effect on MMP2, MMP9 and Snail1 (Fig. 7c). Therefore, we speculated that MAY inhibited EMT through targeting Twist1 in A549/Taxol cells.

4. Discussion

Lung cancer has the highest morbidity and mortality among malignant tumors. Among them, more than 80% of lung cancer patients are NSCLC [33]. Although paclitaxel is the commonly used drug for NSCLC treatment, increased drug-resistance limits its clinical use [34]. Drug-resistant NSCLC leads to poor outcome due to lack of further effective drugs [35]. In this study, we found that MAY inhibited microtubule polymerization and induced G2/M phase arrest in A549 and A549/Taxol cells. Furthermore, MAY induced apoptosis through the mitochondrial pathway in A549 cells and through the extrinsic pathway in A549/Taxol cells. Our research shows that MAY is a promising anticancer drug for NSCLC.

Due to the complex mechanism of MDR, understanding its mechanism is necessary to overcome chemotherapy resistance in NSCLC cells. ABC transporters overexpress in most drug-resistant cancers and

protect tumor cells by reducing intracellular drug concentration [36]. P-gp is a typical ABC transporter in drug-resistant tumor cells and has multiple functions and substrates [37]. In this study, we found that highly expressed P-gp was the main factor of chemoresistance in A549/Taxol cells. In addition, MAY was not a substrate for P-gp and inhibited the expression and function of P-gp.

EMT is an important process in the malignant development of tumors and can promote tumors metastasis [38]. Studies have shown that EMT can be regulated by a variety of cytokines and growth factors [15]. In the presence of EMT, epithelial cells gradually obtain mesenchymal phenotype and enhance migration and invasion abilities [39]. In this study, we discovered that the resistant NSCLC cells acquired mesenchymal-like phenotype and displayed greater motility. Simultaneously, the expression levels of epithelial markers were decreased and the expression levels of mesenchymal markers were increased in A549/Taxol cells compared with A549 cells.

Studies have reported that a variety of transcription factors were participated in the regulation of EMT, including Twist1, Snail1 and Slug [29,40]. Twist1, a member of zinc-finger transcription factor, is the most important adjustment factor of EMT [41]. Many studies have shown that Twist1 inhibits E-cadherin transcription through binding to the E-box site in the E-cadherin promoter [42,43]. In addition, Twist1 not only promotes the EMT process, but also enhances drug resistance [44]. In this study, MAY inhibited the expression of Twist1 and led to the inhibition of migration and invasion in A549/Taxol cells.

In conclusion, MAY inhibits microtubule polymerization and induces G2/M phase arrest in A549 and A549/Taxol cells. Furthermore, MAY induces apoptosis in A549 and A549/Taxol cells. These results indicate that MAY is a promising anticancer drug for NSCLC. In addition, we find that highly expressed P-gp is the main factor of chemoresistance in A549/Taxol cells. Importantly, MAY is not a P-gp substrate, and it can inhibit P-gp expression and function in A549/Taxol cells. Besides, MAY inhibits EMT by targeting Twist1 in A549/Taxol cells. Our findings suggest that MAY could provide a promising method for the treatment of NSCLC, especially for the treatment of resistant NSCLC.

CRediT authorship contribution statement

Jianan Du: Methodology, Formal analysis, Investigation, Writing - original draft, Writing - review & editing. **Jingnan Li:** Methodology, Resources, Formal analysis. **Minghuan Gao:** Methodology, Resources, Formal analysis. **Qi Guan:** Methodology, Resources. **Tong Liu:** Methodology, Resources, Formal analysis. **Yue Wu:** Methodology, Resources. **Zengqiang Li:** Software, Resources. **Daiying Zuo:** Conceptualization, Project administration, Supervision, Writing - review & editing. **Weige Zhang:** Project administration, Supervision. **Yingliang Wu:** Project administration, Supervision.

Declaration of competing interest

The authors declare that they have no known competing financial interests or personal relationships that could have appeared to influence the work reported in this paper.

Acknowledgement

We gratefully acknowledge the National Natural Science Foundation of China (81872394 and 81673293) and Liaoning Revitalization Talents Program of China (XLYC1802072) for the generous financial support.

Appendix A. Supplementary data

Supplementary data to this article can be found online at https://doi.org/10.1016/j.cbi.2020.109074.

References

[1] R.L. Siegel, K.D. Miller, A. Jemal, Cancer statistics, 2019, CA A Cancer J. Clin. 69 (1) (2019) 7–34.
[2] R.L. Siegel, K.D. Miller, A. Jemal, Cancer statistics, 2018, CA A Cancer J. Clin. 68 (1) (2018) 7–30.
[3] R.L. Siegel, K.D. Miller, A. Jemal, Cancer statistics, 2017, CA A Cancer J. Clin. 67 (1) (2017) 7–30.
[4] L.A. Torre, R.L. Siegel, A. Jemal, Lung cancer statistics, Adv. Exp. Med. Biol. 893 (2016) 1–19.
[5] Z. Bai, et al., BZML, a novel colchicine binding site inhibitor, overcomes multidrug resistance in A549/Taxol cells by inhibiting P-gp function and inducing mitotic catastrophe, Canc. Lett. 402 (2017) 81–92.
[6] F. Wu, et al., The role of Axl in drug resistance and epithelial-to-mesenchymal transition of non-small cell lung carcinoma, Int. J. Clin. Exp. Pathol. 7 (10) (2014) 6653–6661.
[7] Y.J. Wang, et al., Regorafenib overcomes chemotherapeutic multidrug resistance mediated by ABCB1 transporter in colorectal cancer: in vitro and in vivo study, Canc. Lett. 396 (2017) 145–154.
[8] M.P. Ceballos, et al., ABC transporters: regulation and association with multidrug resistance in hepatocellular carcinoma and colorectal carcinoma, Curr. Med. Chem. 26 (7) (2019) 1224–1250.
[9] M. Zhou, et al., Overcoming chemotherapy resistance via simultaneous drug-efflux circumvention and mitochondrial targeting, Acta Pharm. Sin. B 9 (3) (2019) 615–625.
[10] A.K. Nanayakkara, P.D. Vogel, J.G. Wise, Prolonged inhibition of P-glycoprotein after exposure to chemotherapeutics increases cell mortality in multidrug resistant cultured cancer cells, PloS One 14 (6) (2019) e0217940.
[11] H. Yin, et al., Design, synthesis and biological evaluation of chalcones as reversers of P-glycoprotein-mediated multidrug resistance, Eur. J. Med. Chem. 180 (2019) 350–366.
[12] W. Guo, et al., Mitochondria P-glycoprotein confers paclitaxel resistance on ovarian cancer cells, OncoTargets Ther. 12 (2019) 3881–3891.
[13] H.Y. Liu, et al., DJ-1 overexpression confers the multidrug resistance phenotype to SGC7901cells by upregulating P-gp and Bcl-2, Biochem. Biophys. Res. Commun. 519 (1) (2019) 73–80.
[14] M. Levi, et al., P-glycoprotein and breast cancer resistance protein in canine inflammatory and noninflammatory grade III mammary carcinomas, Vet. Pathol. 56 (6) (2019) 840–847 300985819868647.
[15] J. Wu, et al., RCCD1 depletion attenuates TGF-beta-induced EMT and cell migration by stabilizing cytoskeletal microtubules in NSCLC cells, Canc. Lett. 400 (2017) 18–29.
[16] V. Odero-Marah, et al., Epithelial-mesenchymal transition (EMT) and prostate cancer, Adv. Exp. Med. Biol. 1095 (2018) 101–110.
[17] W. Gou, et al., CD74-ROS1 G2032R mutation transcriptionally up-regulates Twist1 in non-small cell lung cancer cells leading to increased migration, invasion, and resistance to crizotinib, Canc. Lett. 422 (2018) 19–28.
[18] Y. Hu, et al., Sabutoclax, pan-active BCL-2 protein family antagonist, overcomes drug resistance and eliminates cancer stem cells in breast cancer, Canc. Lett. 423 (2018) 47–59.
[19] M. Lim, et al., Targeting metabolic flexibility via angiopoietin-like 4 protein sensitizes metastatic cancer cells to chemotherapy drugs, Mol. Canc. 17 (1) (2018) 152.
[20] M. Saxena, et al., Transcription factors that mediate epithelial-mesenchymal transition lead to multidrug resistance by upregulating ABC transporters, Cell Death Dis. 2 (2011) e179.
[21] W. Li, et al., Overexpression of Snail accelerates adriamycin induction of multidrug resistance in breast cancer cells, Asian Pac. J. Cancer Prev. APJCP 12 (10) (2011) 2575–2580.
[22] K. Zhu, et al., Short hairpin RNA targeting Twist1 suppresses cell proliferation and improves chemosensitivity to cisplatin in HeLa human cervical cancer cells, Oncol. Rep. 27 (4) (2012) 1027–1034.
[23] E. Mato, et al., ABCG2/BCRP gene expression is related to epithelial-mesenchymal transition inducer genes in a papillary thyroid carcinoma cell line (TPC-1), J. Mol. Endocrinol. 52 (3) (2014) 289–300.
[24] Y. Wu, et al., Design and synthesis of 5-aryl-4-(4-arylpiperazine-1-carbonyl)-2H-1,2,3-triazole derivatives as colchicine binding site inhibitors, Sci. Rep. 7 (1) (2017) 17120.
[25] M. Han, et al., 5-chloro-N4-(2-(isopropylsulfonyl)phenyl)-N2-(2-methoxy-4-(4-((4-methylpiperazin-1-yl)methyl)-1H-1,2,3-triazol-1-yl)phenyl)pyrimidine-2,4-diamine (WY-135), a novel ALK inhibitor, induces cell cycle arrest and apoptosis through inhibiting ALK and its downstream pathways in Karpas299 and H2228cells, Chem. Biol. Interact. 284 (2018) 24–31.
[26] A. Nahata, et al., Sphaeranthus indicus induces apoptosis through mitochondrial-dependent pathway in HL-60 cells and exerts cytotoxic potential on several human cancer cell lines, Integr. Canc. Ther. 12 (3) (2013) 236–247.
[27] F. Liu, et al., The novel nature microtubule inhibitor ivalin induces G2/M arrest and apoptosis in human hepatocellular carcinoma SMMC-7721 cells in vitro, Medicina 55 (8) (2019).
[28] W. Li, et al., Synthesis, molecular properties prediction and biological evaluation of indole-vinyl sulfone derivatives as novel tubulin polymerization inhibitors targeting the colchicine binding site, Bioorg. Chem. 85 (2019) 49–59.
[29] T. Tomono, K. Yano, T. Ogihara, Snail-induced epithelial-to-mesenchymal transition enhances P-gp-Mediated multidrug resistance in HCC827 cells, J. Pharmacol.

Sci. 106 (9) (2017) 2642–2649.
[30] Z.A. Yochum, et al., Targeting the EMT transcription factor TWIST1 overcomes resistance to EGFR inhibitors in EGFR-mutant non-small-cell lung cancer, Oncogene 38 (5) (2019) 656–670.
[31] I.T. Tsai, et al., Novel microtubule inhibitor MPT0B098 inhibit shypoxia-induced epithelial-to- mesenchymal transition in head and neck squamous cell carcinoma, J. Biomed. Sci. 25 (1) (2018) 28.
[32] H. Lu, et al., Novel ADAM-17 inhibitor ZLDI-8 inhibits the proliferation and metastasis of chemo-resistant non-small-cell lung cancer by reversing Notch and epithelial mesenchymal transition in vitro and in vivo, Pharmacol. Res. 148 (2019) 104406.
[33] H. Lu, et al., Novel ADAM-17 inhibitor ZLDI-8 inhibits the proliferation and metastasis of chemo-resistant non-small-cell lung cancer by reversing Notch and epithelial mesenchymal transition in vitro and in vivo, Pharmacol. Res. 148 (2019) 104406.
[34] D.S. Metzinger, D.D. Taylor, C. Gercel-Taylor, Induction of p53 and drug resistance following treatment with cisplatin or paclitaxel in ovarian cancer cell lines, Canc. Lett. 236 (2) (2006) 302–308.
[35] X. Xie, et al., Overcoming drug-resistant lung cancer by paclitaxel loaded tetrahedral DNA nanostructures, Nanoscale 10 (12) (2018) 5457–5465.
[36] M. Kairuki, et al., Designed P-glycoprotein inhibitors with triazol-tetrahydroisoquinoline-core increase doxorubicin-induced mortality in multidrug resistant K562/A02 cells, Bioorg. Med. Chem. 27 (15) (2019) 3347–3357.
[37] S. Mollazadeh, et al., Synthesis, in silico and in vitro studies of new 1,4-dihydropiridine derivatives for antitumor and P-glycoprotein inhibitory activity, Bioorg. Chem. 91 (2019) 103156.
[38] J. Lee, J.H. Choi, C.K. Joo, TGF-beta1 regulates cell fate during epithelial-mesenchymal transition by upregulating survivin, Cell Death Dis. 4 (2013) e714.
[39] J.J. Deng, et al., Twist mediates an aggressive phenotype in human colorectal cancer cells, Int. J. Oncol. 48 (3) (2016) 1117–1124.
[40] J. Yao, et al., ABCB5-ZEB1 Axis promotes invasion and metastasis in breast cancer cells, Oncol. Res. 25 (3) (2017) 305–316.
[41] C.H. Kwon, et al., TWIST mediates resistance to paclitaxel by regulating Akt and Bcl-2 expression in gastric cancer cells, Tumour Biol 39 (10) (2017) 1010428317722070.
[42] Y. Li, et al., CASC15 promotes epithelial to mesenchymal transition and facilitates malignancy of hepatocellular carcinoma cells by increasing TWIST1 gene expression via miR-33a-5p sponging, Eur. J. Pharmacol. 860 (2019) 172589.
[43] C.Y. Yu, et al., HR23A-knockdown lung cancer cells exhibit epithelial-to-mesenchymal transition and gain stemness properties through increased Twist1 stability, Biochim. Biophys. Acta Mol. Cell Res. 1866 (12) (2019) 118537.
[44] W.J. Chen, et al., Multidrug resistance in breast cancer cells during epithelial-mesenchymal transition is modulated by breast cancer resistant protein, Chin. J. Canc. 29 (2) (2010) 151–157.